MOLECULAR AND CELLULAR BIOLOGY, May 2004, p. 3949–3956 Vol. 24, No. 9
0270-7306/04/$08.00+0 DOI: 10.1128/MCB.24.9.3949–3956.2004

Ndrg1-Deficient Mice Exhibit a Progressive Demyelinating Disorder of Peripheral Nerves

Tomohiko Okuda,[1] Yujiro Higashi,[2] Koichi Kokame,[1] Chihiro Tanaka,[1] Hisato Kondoh,[2] and Toshiyuki Miyata[1]*

National Cardiovascular Center Research Institute, Suita, Osaka 565-8565,[1] and Laboratory of Developmental Biology, Graduate School of Frontier Bioscience, Osaka University, Suita, Osaka 565-0871,[2] Japan

Received 28 August 2003/Returned for modification 3 November 2003/Accepted 10 January 2004

NDRG1 is an intracellular protein that is induced under a number of stress and pathological conditions, and it is thought to be associated with cell growth and differentiation. Recently, human *NDRG1* was identified as a gene responsible for hereditary motor and sensory neuropathy-Lom (classified as Charcot-Marie-Tooth disease type 4D), which is characterized by early-onset peripheral neuropathy, leading to severe disability in adulthood. In this study, we generated mice lacking *Ndrg1* to analyze its function and elucidate the pathogenesis of Charcot-Marie-Tooth disease type 4D. Histological analysis showed that the sciatic nerve of *Ndrg1*-deficient mice degenerated with demyelination at about 5 weeks of age. However, myelination of Schwann cells in the sciatic nerve was normal for 2 weeks after birth. *Ndrg1*-deficient mice showed muscle weakness, especially in the hind limbs, but complicated motor skills were retained. In wild-type mice, NDRG1 was abundantly expressed in the cytoplasm of Schwann cells rather than the myelin sheath. These results indicate that NDRG1 deficiency leads to Schwann cell dysfunction, suggesting that NDRG1 is essential for maintenance of the myelin sheaths in peripheral nerves. These mice will be used for future analyses of the mechanisms of myelin maintenance.

NDRG1, an intracellular protein composed of 394 amino acids, is highly conserved among multicellular organisms, and its expression is induced by stress stimuli. Previously, we showed that NDRG1 is induced by homocysteine, 2-mercaptoethanol, and tunicamycin in cultured human endothelial cells (13). This pattern is similar to that seen for molecular chaperones in the endoplasmic reticulum. Subsequently, NDRG1 was found to be upregulated in a human lung cells following treatment with nickel compounds (31). This change in expression reflected an increase in hypoxia-inducible factor 1 caused by hypoxia or the subsequent elevation of intercellular calcium concentrations (23, 24). NDRG1 expression is also induced by p53 expression and DNA damage, and its expression is inhibited under conditions of cell growth (14). These results suggest that NDRG1 is involved in the cellular stress response mechanisms.

Conversely, *Ndrg1* was also identified as a downstream target of N-*myc* (25). In N-*myc* knockout mouse embryos, NDRG1 expression is upregulated. During the early stages of differentiation of some tissues, it seems that N-myc activity leads to decreased NDRG1 expression as tissue differentiation progresses. Indeed, *NDRG1* has been identified as a gene whose expression is downregulated in tumors (14, 27). Furthermore, NDRG1 expression is induced by differentiation stimuli in cancer cells (21, 29). *NDRG1* was also reported to be a metastasis suppressor gene (3, 6). In this regard, the effects of *NDRG1* are thought to reflect its potential role in cell differentiation.

Recently, a nonsense mutation of human *NDRG1* was reported to be causative for hereditary motor and sensory neuropathy-Lom (9), which is a severe peripheral neuropathy identified in the Gypsy community of Lom, a small town in northwest Bulgaria (10, 11). The hereditary motor and sensory neuropathy-Lom is classified as Charcot-Marie-Tooth disease type 4D (4). Patients with this disease exhibit an early-onset peripheral neuropathy that progresses to severe disability in adulthood, characterized by muscle weakness, sensory loss, and neural deafness. These symptoms are caused by demyelination of peripheral nerves. These observations suggest that NDRG1 is necessary for axonal survival.

To clarify the function(s) of NDRG1, we generated *Ndrg1*-deficient mice by gene targeting. The *Ndrg1*-deficient mice exhibited progressive demyelination in peripheral nerves. Moreover, we showed that NDRG1 was significantly expressed in the cytoplasm of Schwann cells, suggesting that NDRG1 deficiency is a primary cause of Schwann cell dysfunction.

MATERIALS AND METHODS

Construction of targeting vector. We isolated genomic clones carrying the mouse *Ndrg1* gene and characterized the promoter and the first exon (25). An 8.9-kb EcoRI fragment encompassing the promoter and exon 1 was used to construct the targeting vector. The initiating Met codon for NDRG1 translation exists in exon 2. A *loxP*-flanked pSTneoB (26) cassette was inserted at the BamHI site 1.2 kb downstream of the transcriptional start site, and an additional *loxP* plus BamHI site sequence was inserted at an EcoRV site 1.2 kb upstream of the start site. This resulted in three *loxP* sites in the vector, so that the Cre recombinase should excise the promoter and exon 1 (Fig. 1A). The sequence was inserted into the diphtheria toxin A fragment cassette vector (30), and the DNA was linearized by SalI digestion for electroporation.

* Corresponding author. Mailing address: National Cardiovascular Center Research Institute, 5-7-1 Fujishirodai, Suita, Osaka 565-8565, Japan. Phone: 81-6-6833-5012, ext. 2512. Fax: 81-6-6835-1176. E-mail: miyata@ri.ncvc.go.jp.

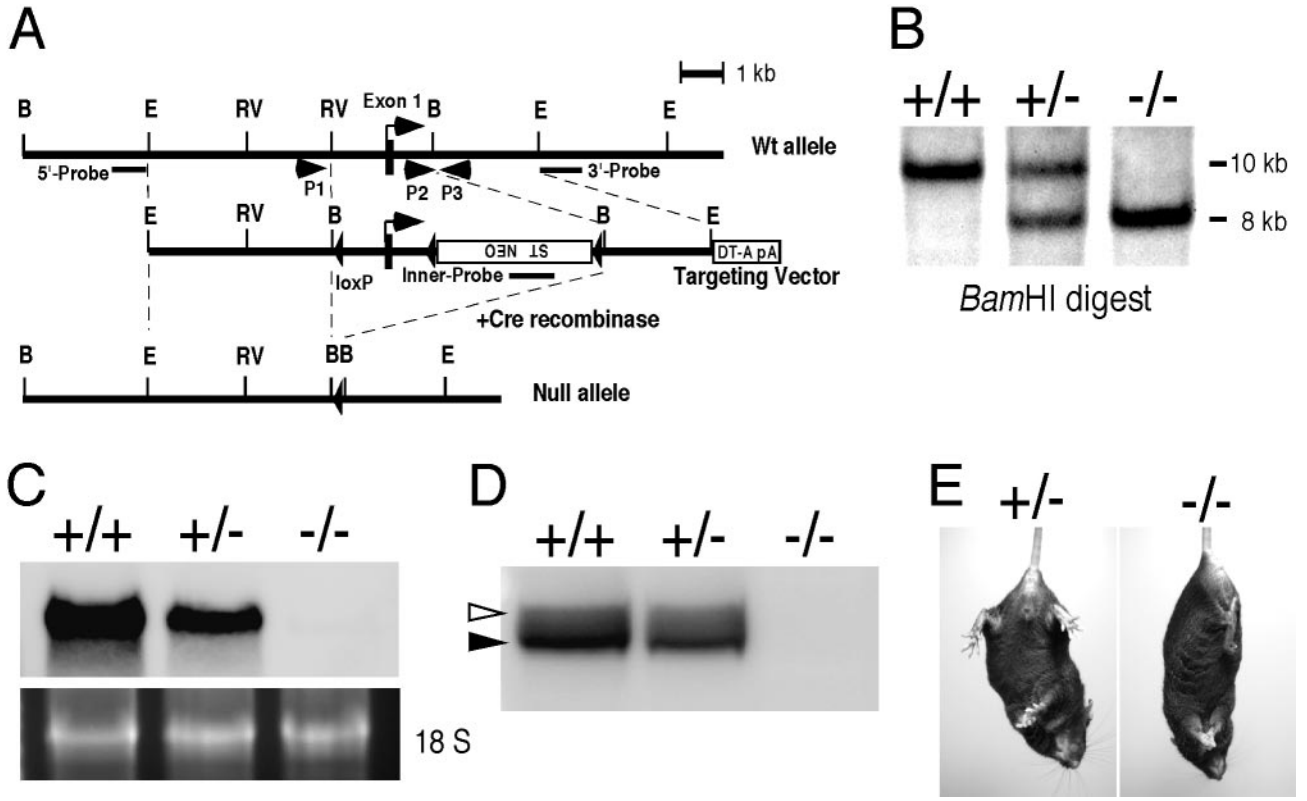

FIG. 1. Targeted disruption of *Ndrg1*. (A) Targeting strategy for the *Ndrg1* gene. Solid boxes represent exon 1 of *Ndrg1*. Arrowheads indicate the location and orientation of *loxP* sites. The *loxP*-flanked pSTneoB cassette (ST NEO) and the third *loxP* sequence were inserted into the targeting vector. A diphtheria toxin A fragment cassette with a polyadenylation signal (DT-A pA) was included at the 3′ end of the vector for negative selection of ES cells. 5′-External, 3′-external, and inner probes for selection of ES clones by Southern blotting are shown as bars. PCR primers to discriminate each allele are shown as P1, P2, and P3. B, BamHI; E, EcoRI; RV, EcoRV. (B) Southern blot analysis. Genomic DNA was prepared from littermates obtained by heterozygous intercrossing and subjected to BamHI digestion. The wild-type and null alleles gave about 10- and 8-kb bands, respectively, with the 5′ probe. (C) Northern blot analysis of the kidneys from 2-month-old male mice. The partial mouse *Ndrg1* cDNA fragment (904 bp) was used as a specific probe. Equal loading among lanes was confirmed by staining of 18 S rRNA. *Ndrg1* mRNA expression was not detected in *Ndrg1*$^{-/-}$ mice. (D) Western blot analysis of the kidneys from 2-month-old male mice. Each lane contains 5 μg of total protein. NDRG1 expression was partially reduced in the *Ndrg1*$^{+/-}$ mouse and absent in the *Ndrg1*$^{-/-}$ mouse. The majority of NDRG1 was detected at an apparent molecular mass of 43 kDa (solid arrowhead). The upper bands indicate phosphorylated NDRG1 (open arrowhead). (E) A phenotype in the appearance of an *Ndrg1*$^{-/-}$ mouse at 3 months of age. An abnormal hind limb clasping phenotype was seen in *Ndrg1*$^{-/-}$ mice upon tail suspension, indicating neurological abnormalities.

Generation of *Ndrg1*-null mutant mice. R1 embryonic stem (ES) cells (18) were electroporated with the targeting vector and selected with 250 μg of G418 per ml. G418-resistant ES colonies were selected, and correctly targeted clones were identified by Southern blotting with a Gene Images Random-Prime system (Amersham Biosciences) with 5′-external, 3′-external, and inner probes (Fig. 1A). These ES cells were injected into blastocysts to obtain mouse chimeras, which were crossed with wild-type C57BL/6 mice (SLC Japan) for germ line transmission of the floxed *Ndrg1* allele. These mice were further crossed with *EIIa-Cre* deleter mice (15) to excise the promoter and exon 1 region of the *Ndrg1* gene together with the neomycin resistance cassette (7). Successful excision of the sequences in the offspring was confirmed by PCR analysis of DNA isolated from punctured ear lobes with primers P1 (5′-AGCAGGCTCTTAAAGCGGC TCC-3′), P2 (5′-CCGCCTCTGTCAAATTAGTAGCTG-3′), and P3 (5′-GGG AGAGCTGAAGGCTGTTCTAGG-3′). Those heterozygous mice with the excised *Ndrg1* allele were backcrossed with wild-type C57BL/6 mice. The heterozygous offspring lacking the *Cre* gene were used for this study. The experiments were conducted in accordance with the current guidelines for the care and use of experimental animals of the National Cardiovascular Center in Japan.

Northern blot analysis. Male mice aged 2 months (wild-type, heterozygous, and homozygous mice) were sacrificed, and their kidneys and sciatic nerves were excised. For extraction of total RNA, whole kidneys or sciatic nerves were immediately homogenized in Trizol reagent (Invitrogen). Isolated total RNA was electrophoresed in a 1% agarose gel containing 2% formaldehyde (10 μg/lane) and transferred to a nylon membrane. To make a specific probe, a partial cDNA fragment (904 bp) was amplified by PCR with primers 5′-CTCAGACA CCAAACTGCCAAAAC-3′ and 5′-AATGCTACAAACCCAGTCAGCAG-3′, with the full-length *Ndrg1* cDNA used as a template. The fragment obtained was labeled with fluorescein-12-dUTP (PerkinElmer Life Sciences), and hybridization and detection procedures were performed as previously described (32).

Western blot analysis. For extraction of total protein, the excised organs were homogenized in lysis buffer as described before (12). The protein lysates were subjected to sodium dodecyl sulfate-polyacrylamide gel electrophoresis (10 to 20% gradient gel) and transferred to a polyvinylidene difluoride membrane (Bio-Rad). After blocking with 3% skim milk in phosphate-buffered saline (PBS) with 0.05% Tween 20, the membrane was incubated with a 1:1,000 dilution of anti-NDRG1 antiserum (2) and then with a 1:1,000 dilution of peroxidase-conjugated goat anti-rabbit immunoglobulin G (Zymed). Detection was performed with the Western Lightning Chemiluminescence Reagent Plus (PerkinElmer Life Sciences) with the LAS-1000plus image analyzer.

Histological analyses. Male mice aged 1, 2, and 5 weeks and 3 and 6 months (wild-type, heterozygous, and homozygous mice) were anesthetized with nembutal (Abbott Laboratories) and perfused with ice-cold PBS containing 4% paraformaldehyde, and sciatic nerve fragments were excised. For light and electron microscopy, the fragments were fixed with 2.5% glutaraldehyde for 2 h at 4°C. After being washed with PBS, the samples were cut into small pieces and fixed with 2% OsO_4 for 2 h at 4°C. After dehydration in an ascending ethanol series, the samples were embedded in Quetol812 resin. For light microscopy, semithin sections (1-μm thickness) of sciatic nerves were stained with 0.1%

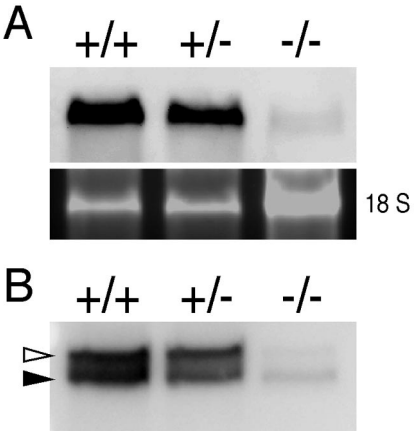

FIG. 2. Leaky expression of NDRG1 in the sciatic nerve of *Ndrg1*$^{-/-}$ mice. (A) Northern blot analysis of the sciatic nerves from mice at 2 months of age. 18 S rRNA was used as an internal control. (B) Western blot analysis of the sciatic nerves from mice at 2 months of age. Each lane contains 5 μg of total protein. NDRG1 was detected at 43 kDa (solid arrowhead). The upper bands indicate phosphorylated NDRG1 (open arrowhead). Low-level expression of NDRG1 was detected in the sciatic nerves of *Ndrg1*$^{-/-}$ mice.

toluidine blue. Slides were examined with an Axioplan 2 microscope (Carl Zeiss). For electron microscopy, ultrathin sections (90-nm thickness) on mesh grids were stained with uranyl acetate and lead acetate and examined with an H-300 electron microscope (Hitachi).

For immunofluorescence microscopy, paraformaldehyde-fixed sciatic nerve specimens from mice aged 3 weeks (wild-type and homozygous mice) were washed with PBS at 4°C and embedded in OCT compound (Sakura Finetek) at −80°C. Frozen sections (5-μm thickness) were washed with PBS. After being blocked with 10% normal goat serum for 15 min at room temperature, the sections were incubated with a 1:200 dilution of anti-NDRG1 antiserum and a 1:100 dilution of rat anti-myelin basic protein (MBP) monoclonal antibody (Chemicon) overnight at 4°C and then with a 1:100 dilution of Alexa Fluor 488-conjugated anti-rabbit immunoglobulin G antibody (Molecular Probes) and a 1:100 dilution of Alexa Fluor 546-conjugated anti-rat immunoglobulin G antibody (Molecular Probes) for 1 h at room temperature. Fluorescence was detected with the Axiovert 200 microscope and photographed with the AxioCam (Carl Zeiss).

Quantitative analysis of demyelination. Semithin sections of sciatic nerves from three homozygous and three wild-type mice aged 3 weeks and 3 months were photographed, and myelinated axons in a fixed area were counted manually. The diameter of the axons and the thickness of nerve fibers (axon plus myelin) were analyzed with ImageGauge software (Fujifilm). To assess the thickness of the myelin sheath, the g ratio (axon diameter/fiber diameter) was calculated (1, 5). Complex figures with folded myelin were excluded. The significance of differences between mean values was determined by the *F* test.

RT-PCR analysis. Total RNA was extracted from the sciatic nerves, kidneys, and brains of homozygous and wild-type mice aged 5 weeks. Reverse transcription-PCR (RT-PCR) was performed with total RNA (50 ng) as the template and a SuperScript One-Step RT-PCR kit with Platinum *Taq* (Invitrogen). The primer pairs were 5′-ACCCTGAGATGGTAGAGGGTCTC-3′ and 5′-CCAATTTAG AATTGCATTCCACC-3′ for *Ndrg1*, 5′-ATTCTTGGACATCTTTTCAGCC A-3′ and 5′-TGCAGGAAGTACTTGAAAGCCTC-3′ for *Ndrg2*, 5′-CATTAA CATTGACCCGTGTGCTA-3′ and 5′-TTGTATTTATAGGGTCGAGGCG A-3′ for *Ndrg3*, 5′-AAGTACGTGATTGGCATTGGAGT-3′ and 5′-CAGGTG CATTATCTCCGACTACC-3′ for *Ndrg4*, and 5′-GGAGAAACCTGCCAAGT ATGATG-3′ and 5′-CTAGGCCCCTCCTGTTATTATGG-3′ for *Gapd*.

Motor activity tests. In the wire-hanging test, we assessed the grip strength of the mice as described before (8). Each mouse was placed on wire netting (20 by 30 cm) taped around the edge. The wire netting was shaken three times and turned upside down. The amount of time that each mouse held onto the wire netting was recorded up to a maximum of 300 s. In the rotorod test, we assessed the ability of the mice to maintain balance on a rotating cylinder as described before (17). The accelerating Rota-Rod (model 7650; Ugo Basile) consists of a 3-cm-diameter cylinder with knurls. Each mouse was placed on the cylinder, which turned at a constant rotation (5 rpm) for 1 min for training, and then the

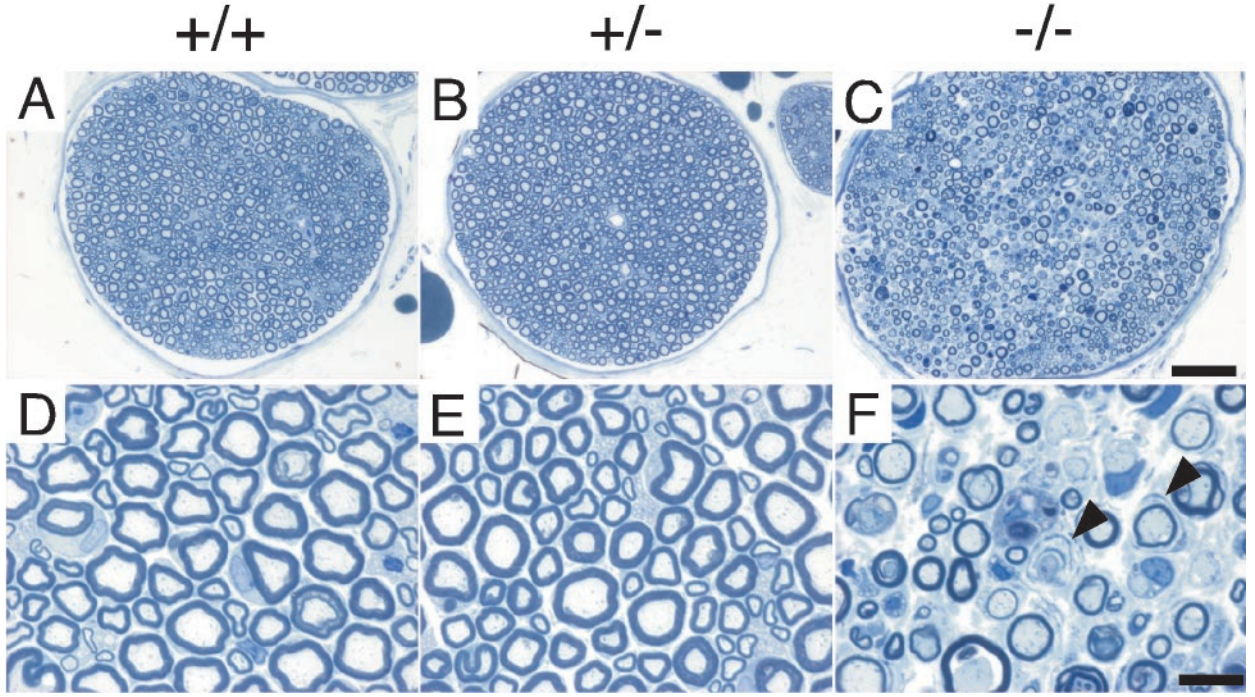

FIG. 3. Histological examination of sciatic nerves. Transverse sections of the sciatic nerves from *Ndrg1*$^{+/+}$ (A and D), *Ndrg1*$^{+/-}$ (B and E), and *Ndrg1*$^{-/-}$ (C and F) mice at 3 months of age are shown. Panels D, E, and F are higher magnifications of panels A, B, and C, respectively. The sciatic nerves of the *Ndrg1*$^{-/-}$ mouse (C and F) showed features typical of demyelinating neuropathy. Many thinly myelinated axons and onion bulb degeneration were seen (arrowheads). No difference was observed between *Ndrg1*$^{+/+}$ and *Ndrg1*$^{+/-}$ mice. Bars, 50 μm (A to C); 10 μm (D to F).

TABLE 1. Quantitative analysis of sciatic nerve[a]

Age	*Ndrg1* genotype	Mean axon density (10^4/mm^2) ± SD	Mean axon diam (μm) ± SD	Mean g ratio ± SD (no. of fibers)
3 wk	+/+	2.65 ± 0.23	3.46 ± 0.97	0.67 ± 0.06 (980)
	−/−	2.87 ± 0.22	3.09 ± 0.82*	0.66 ± 0.06 (1,028)
3 mo	+/+	2.45 ± 0.32	4.13 ± 1.41	0.67 ± 0.06 (760)
	−/−	1.61 ± 0.12*	3.19 ± 1.09*	0.73 ± 0.09* (661)

[a] *, statistically different from *Ndrg1*$^{+/+}$ mice of the same age ($P < 0.05$).

rotation speed was increased over a 300-s period from 5 to 30 rpm. The amount of time that the mouse remained on the accelerating cylinder was recorded. Mice that fell in less than 15 s were given a second trial. Mice that did not fall during the 300-s trial period were given a score of 300 s. Two sets of the rotorod test were performed in the same day, and the higher score for each mouse is reported. The body weight of each mouse was also measured. Both motor activity tests were carried out once every 2 weeks from 5 to 19 weeks of age.

RESULTS

Generation of *Ndrg1*-deficient mice. We made a targeting vector to eliminate *Ndrg1* expression by deletion of the promoter and exon 1 region with *Cre-loxP* excision (Fig. 1A). R1 ES cells were electroporated with the targeting vector and selected with G418. One hundred forty-five G418-resistant ES colonies were selected, and correctly targeted clones were identified by Southern blotting with a 5′-external sequence probe (Fig. 1A and B). Five independently targeted clones were isolated, and the genomic organization of their *Ndrg1* locus was further confirmed by Southern blotting with 3′-external and internal probes. After *Cre-loxP* excision, two lines of mice heterozygous for deletion of the *Ndrg1* promoter and exon 1 were obtained. Mice with the deleted *Ndrg1* allele and without the *Cre* gene (*Ndrg1*$^{+/-}$) were backcrossed with wild-type C57BL/6 mice (*Ndrg1*$^{+/+}$). The *Ndrg1*$^{+/-}$ mice were crossed to generate homozygous *Ndrg1*-deficient mice (*Ndrg1*$^{-/-}$).

Phenotype of *Ndrg1*-deficient mice. *Ndrg1*$^{-/-}$ mice were born normally with the expected Mendelian frequency. Both male and female *Ndrg1*$^{-/-}$ mice were fertile. We confirmed the elimination of NDRG1 expression in the kidney, where NDRG1 was abundantly expressed in wild-type mice (Fig. 1C and D) (32). However, in the sciatic nerve, a faint signal of *Ndrg1* mRNA was detectable in *Ndrg1*$^{-/-}$ mice by Northern blot analysis (Fig. 2A). Leaky transcription of NDRG1 might be possible because the *Ndrg1*$^{-/-}$ mice still showed normal organization of the *Ndrg1* gene downstream of exon 2, containing the initiating Met codon. To confirm this possibility, we performed Western blot analysis on lysates from the sciatic nerves of *Ndrg1*$^{+/+}$, *Ndrg1*$^{+/-}$, and *Ndrg1*$^{-/-}$ mice. As shown in Fig. 2B, faint bands corresponding to the normal size of NDRG1 were observed. These data suggested that a small amount of full-length NDRG1 was expressed in the sciatic nerves of *Ndrg1*$^{-/-}$ mice. In this regard, *Ndrg1*$^{-/-}$ mice are hypomorphic, at least in the sciatic nerves.

Despite the low-level expression of NDRG1, *Ndrg1*$^{-/-}$ mice began showing hind limb weakness at 3 months of age. We also detected an abnormal limb clasping phenotype in *Ndrg1*$^{-/-}$ mice upon tail suspension (Fig. 1E). These observations suggested neurological abnormalities. These phenotypes were progressive, that is, 1-year-old or older *Ndrg1*$^{-/-}$ mice exhibited substantial impairment in hind limb function (i.e., dragging of their legs) and leg muscle atrophy. Two independent lines of *Ndrg1*$^{-/-}$ mice exhibited similar phenotypes. *Ndrg1*$^{+/-}$ mice were indistinguishable from *Ndrg1*$^{+/+}$ mice in both appearance and behavior.

Peripheral nerve degeneration of *Ndrg1*-deficient mice. To address possible peripheral nerve dysfunction, we performed histological analyses. Severe degeneration of the sciatic nerves in *Ndrg1*$^{-/-}$ mice was seen at 3 months of age. We observed a large number of thinly myelinated axons (Fig. 3C and F). The myelinated axons were significantly decreased in density, and the g ratios of the neuronal fibers were significantly increased in *Ndrg1*$^{-/-}$ mice at 3 months of age (Table 1). Electron microscopy of the sciatic nerve showed onion bulb pathology with Schwann cell processes, thin myelin sheaths, endoneurial collagenization, and infiltration of macrophages in *Ndrg1*$^{-/-}$ mice (Fig. 4C). A similar demyelinating phenotype is seen in human Charcot-Marie-Tooth disease type 4D patients (11).

To investigate the process of demyelination in *Ndrg1*$^{-/-}$ mice, we assessed the initial formation of the neuronal myelin sheath at a younger age. Histological analysis showed that, at 1 and 2 weeks of age, the sciatic nerves of *Ndrg1*$^{-/-}$ mice did not differ from the nerves of *Ndrg1*$^{+/+}$ mice; both displayed normal

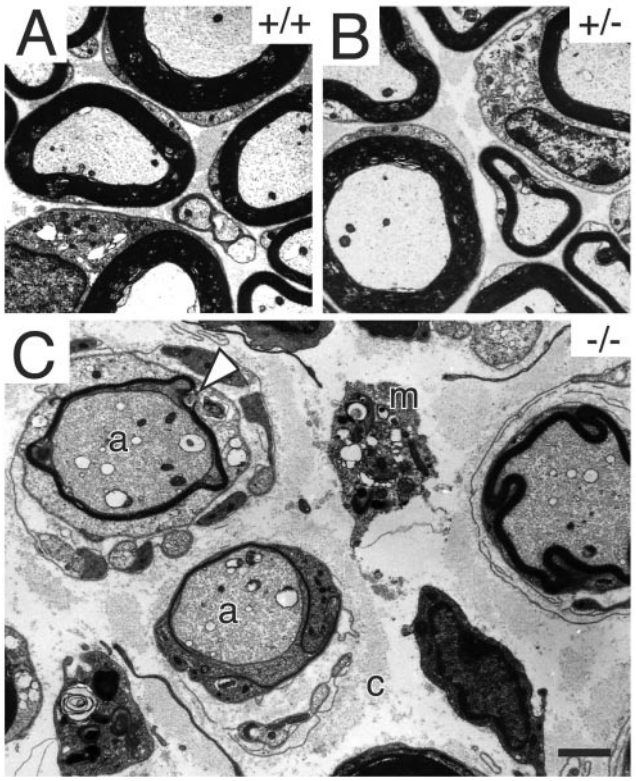

FIG. 4. Electron microscopy of sciatic nerves. Electron micrographs of the sciatic nerves from *Ndrg1*$^{+/+}$ (A), *Ndrg1*$^{+/-}$ (B), and *Ndrg1*$^{-/-}$ (C) mice at 3 months of age were shown. Onion bulb pathology with Schwann cell processes (*open arrowhead*), axons with thin myelin sheath (a), excess collagenization (c), and infiltration of macrophages (m) were observed in *Ndrg1*$^{-/-}$ mice. Bar, 2 μm.

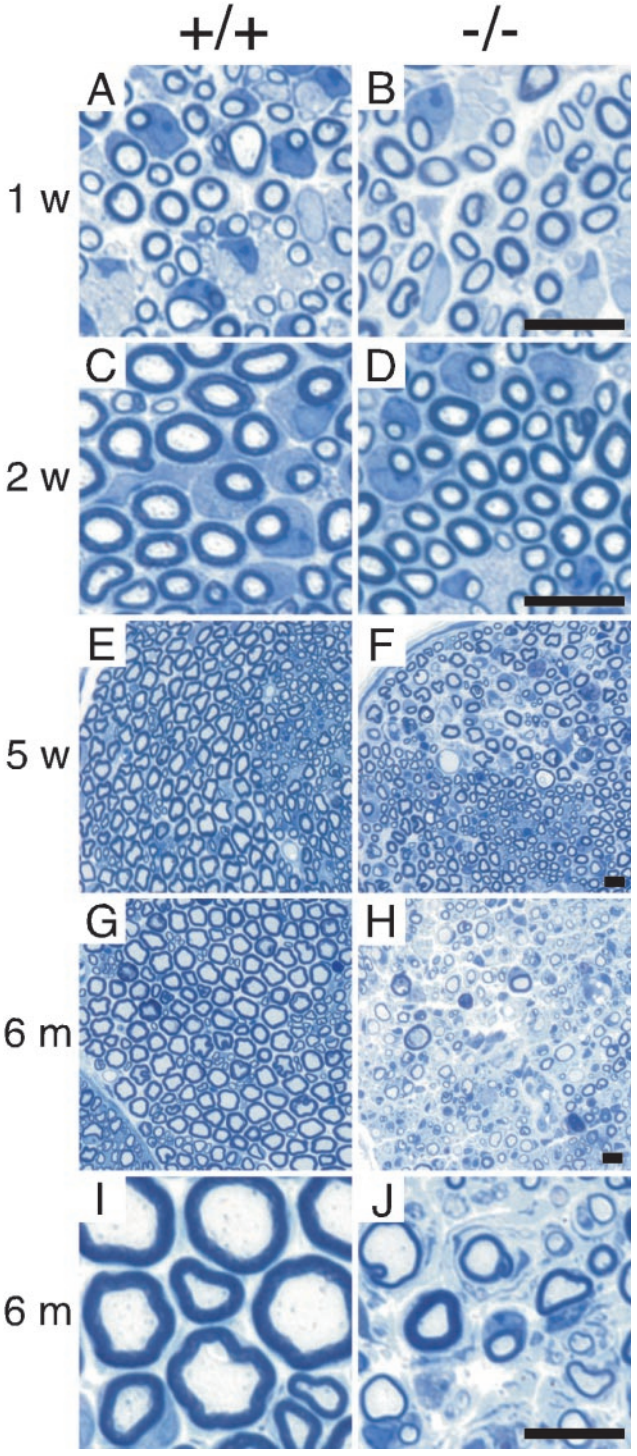

FIG. 5. Time course analysis of sciatic nerves during growth. Transverse sections of the sciatic nerves from *Ndrg1*$^{+/+}$ (A, C, E, G, and I) and *Ndrg1*$^{-/-}$ (B, D, F, H, and J) mice were compared. These specimens were derived from mice of the following ages: A and B, 1 week; C and D, 2 weeks; E and F, 5 weeks; and G to J, 6 months. Panels I and J are higher magnifications of panels G and H, respectively. At 1 to 2 weeks of age, Schwann cell proliferation and myelin formation were normal, and no demyelination was observed in *Ndrg1*$^{-/-}$ mice. However, at 5 weeks of age, partial degeneration of the sciatic nerves had occurred in *Ndrg1*$^{-/-}$ mice, especially in relatively thick axons. At 6 months of age, degeneration of the sciatic nerves had progressed further, with an apparent reduction of myelinated axons in *Ndrg1*$^{-/-}$ mice. Bars, 10 μm.

growth of Schwann cells and normal formation of the myelin sheath (Fig. 5A to D). At 3 weeks of age, the density of myelinated axons was not affected in *Ndrg1*$^{-/-}$ mice, and no significant difference in the g ratios was observed (Table 1). However, at 5 weeks of age, the myelin sheaths of *Ndrg1*-deficient mice began to degenerate (Fig. 5F). The observed demyelination was incomplete and sporadic but was especially pronounced in the myelin sheaths of relatively thick axons. These results indicated that Schwann cell proliferation and myelination were normal and that some defect in the maintenance of the myelin sheath occurred in *Ndrg1*$^{-/-}$ mice. Older *Ndrg1*$^{-/-}$ mice exhibited more severe disease in their sciatic nerves, demonstrating that this peripheral nerve degeneration is progressive (Fig. 5G to J).

NDRG1 is ubiquitously expressed in various tissues (13, 32). In particular, the kidney is reported to be a site of high NDRG1 expression in mice and humans (16, 32). Although the peripheral nerves of *Ndrg1*$^{-/-}$ mice demonstrated clear pathology, no apparent morphological abnormality was observed in their kidneys (data not shown).

Localization of NDRG1 protein in the sciatic nerve. To examine which cells, neurons or Schwann cells, are responsible for the demyelinating defects, we investigated the expression of NDRG1 in the sciatic nerve by immunohistochemical analysis. At 3 weeks of age, NDRG1 was abundantly expressed in the cytoplasm of Schwann cells rather than in myelin sheaths or axons in *Ndrg1*$^{+/+}$ mice (Fig. 6A to C). We confirmed that MBP, a myelin marker protein, was normally expressed in the myelin sheath of the sciatic nerves of both *Ndrg1*$^{+/+}$ and *Ndrg1*$^{-/-}$ mice (Fig. 6B and E). These results suggested that the cytoplasmic expression of NDRG1 in Schwann cells is essential for the maintenance of myelin structure. Thus, defects in Schwann cells caused by NDRG1 deficiency could be a primary cause of the neural degeneration seen in *Ndrg1*$^{-/-}$ mice.

Expression of other NDRG family members. To compare the expression patterns of all NDRG family members, we performed RT-PCR analysis on RNA samples from the sciatic nerve, brain, and kidney of *Ndrg1*$^{+/+}$ and *Ndrg1*$^{-/-}$ mice (Fig. 7). In *Ndrg1*$^{+/+}$ mice, *Ndrg1* was expressed in the sciatic nerves as much as in the kidney but relatively less expressed in the brain. In contrast, *Ndrg2*, *Ndrg3*, and *Ndrg4* were abundantly expressed in the brain of both *Ndrg1*$^{+/+}$ and *Ndrg1*$^{-/-}$ mice but less in the sciatic nerves. Upregulation of *Ndrg2*, *Ndrg3*, and *Ndrg4* was not observed in *Ndrg1*$^{-/-}$ mice.

Muscle strength and motor activity of *Ndrg1*-deficient mice. To examine the muscle strength of the legs, the wire-hanging test was performed. *Ndrg1*$^{-/-}$ mice were able to hang onto the wire for a significantly shorter period than *Ndrg1*$^{+/+}$ at all ages tested. *Ndrg1*$^{-/-}$ mice demonstrated that their muscle strength was quite decreased. Male mice of both genotypes tended to fall sooner than females due to their heavier body weight (Fig. 8A and C). To measure more complicated motor activities and motor learning in the same mice, a rotorod test was carried out. The scores of older *Ndrg1*$^{-/-}$ mice in this test were slightly lower than those of the age-matched *Ndrg1*$^{+/+}$ controls, though the differences were minor compared to those seen in the wire-hanging test (Fig. 8B).

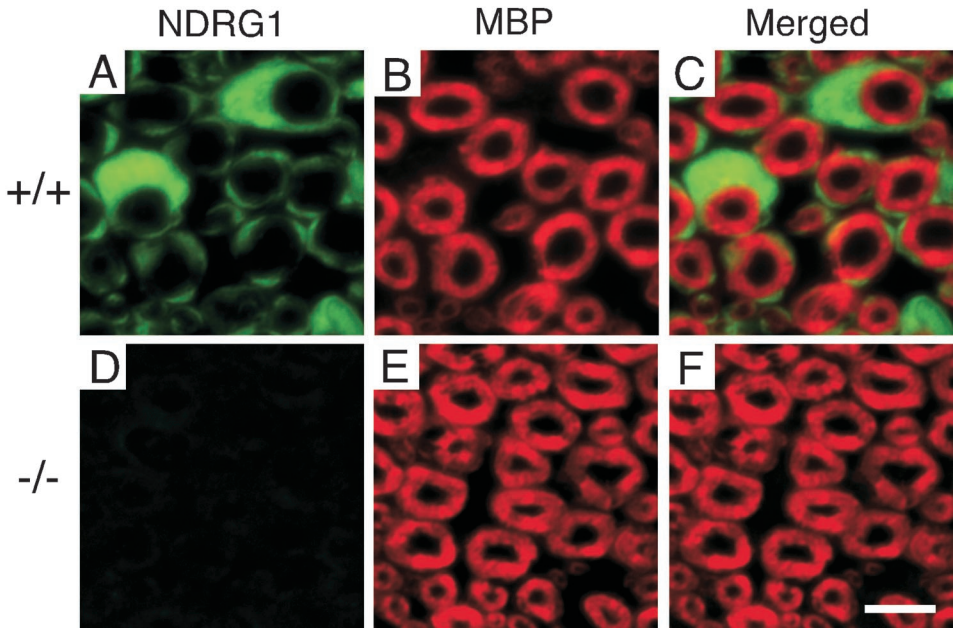

FIG. 6. Immunofluorescence analysis of sciatic nerves. Transverse sections of the sciatic nerves from mice at 3 weeks of age were double stained with anti-NDRG1 antiserum (green; A and D) and anti-MBP antibody (red; B and E). Sections from *Ndrg1*$^{+/+}$ (A to C) and *Ndrg1*$^{-/-}$ (D to F) mice were compared. The merged images are shown in panels C and F. Bar, 10 μm.

DISCUSSION

In this study, we successfully generated *Ndrg1*$^{-/-}$ mice. The *Ndrg1*$^{-/-}$ mice exhibited a progressive demyelinating disorder of the peripheral nerves. Histological and quantitative analyses revealed that Schwann cell proliferation and the initial myelination of *Ndrg1*$^{-/-}$ mice were normal after birth (Fig. 5 and Table 1). However, sporadic degeneration began by 5 weeks of age (Fig. 5). These results strongly suggest that the ability to form myelin sheaths is retained but some defect in the maintenance of the myelin sheath is present in the Schwann cells of *Ndrg1*$^{-/-}$ mice. Therefore, NDRG1 is essential for maintenance of the myelin sheath.

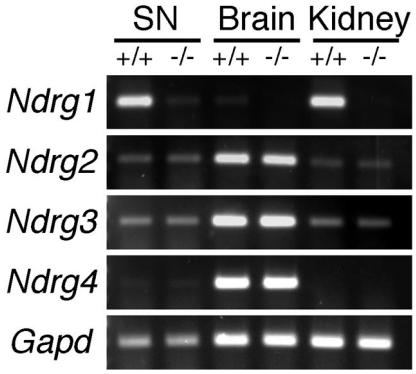

FIG. 7. mRNA expression of *Ndrg* family members. RT-PCR analysis was performed on total RNA samples from the sciatic nerves, brains, and kidneys of *Ndrg1*$^{+/+}$ and *Ndrg1*$^{-/-}$ mice at 5 weeks of age. In *Ndrg1*$^{+/+}$ mice, *Ndrg1* was expressed in the sciatic nerve as much as in the kidney. In contrast, *Ndrg2*, *Ndrg3*, and *Ndrg4* were abundantly expressed in the brain but less in the sciatic nerve. Expression of *Gapd* was examined as an internal control. SN, sciatic nerve.

It has been reported that NDRG1 expression is induced by differentiation or stress stimuli (21, 27, 29). NDRG1 has also been proposed to shuttle between the cytoplasm and the nucleus in cells (14). Furthermore, phosphorylation of NDRG1 depends on extracellular stimuli (2). These observations imply that NDRG1 may have a role in signal transduction. Recently, it was reported that rat NDRG1 is expressed in astrocytes only in the regions where neurons existed (28). This observation suggests that NDRG1 may also play a similar role in neuronal survival in the brain. We demonstrated that NDRG1 was abundantly expressed in the Schwann cell cytoplasm rather than in myelin sheaths (Fig. 6). This expression pattern is unique compared to that of other Charcot-Marie-Tooth disease-responsible proteins, such as peripheral myelin protein 22, myelin protein zero, connexin 32, and L-periaxin (4). These proteins are localized to the plasma membrane of Schwann cells and are thought to have a role in the formation and/or stabilization of the myelin sheaths. Cytoplasmic expression and phosphorylation of NDRG1 implies its association with intracellular signal transduction in Schwann cells. The NDRG1-mediated signals in Schwann cells related to axonal cross talk could be important for the maintenance of myelin sheaths and axonal survival.

Ndrg1$^{-/-}$ mice exhibited muscle weakness, whereas the complicated motor abilities were relatively retained (Fig. 8). These results indicate that NDRG1 deficiency causes peripheral nerve degeneration leading to muscle weakness. This suggests that peripheral nerves may be quite vulnerable to NDRG1 deficiency but that some degree of functional redundancy for NDRG1 may exist within the central nervous system. NDRG1 is one of four NDRG family members exhibiting different expression patterns (20, 22, 32). We previously demonstrated that NDRG4 is abundantly expressed in neurons in the brain but not in the peripheral nerves (32). NDRG4 ex-

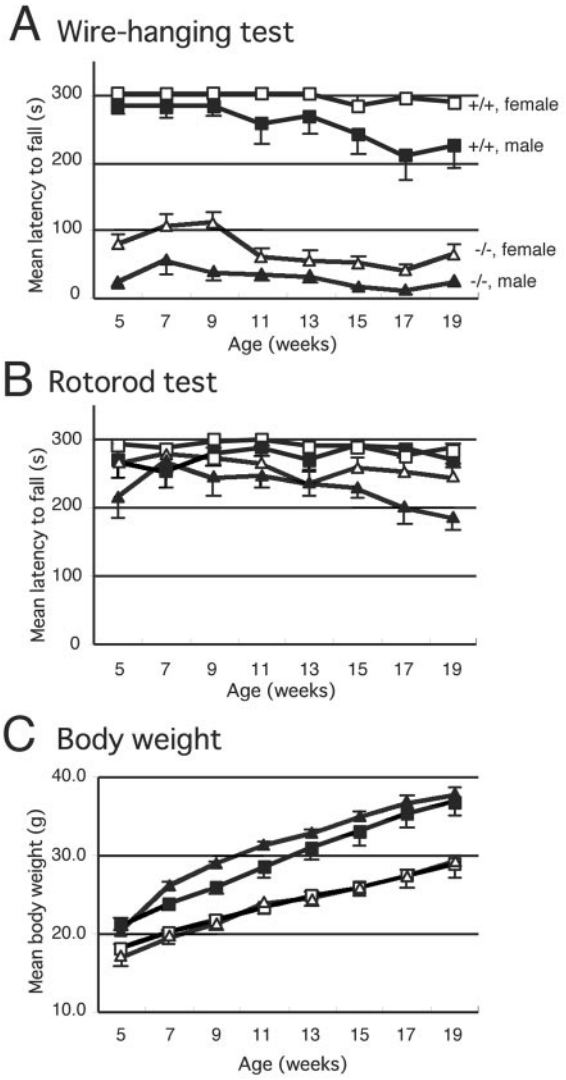

FIG. 8. Assessment of motor activity of *Ndrg1*$^{-/-}$ mice. (A) The wire-hanging test was carried out to measure the grip strength of *Ndrg1*$^{+/+}$ (seven males and seven females) and *Ndrg1*$^{-/-}$ (seven males and six females) mice. The time that each mouse held onto the wire netting was recorded up to a maximum of 300 s. The mean (± standard error of the mean) time before the mouse fell off is shown. (B) The rotorod test was carried out to measure more complicated motor activities in the same mice. The time that each mouse held onto the accelerating cylinder was recorded up to a maximum of 300 s. Mean (±standard error of the mean) time before the mouse fell off the cylinder is shown. Although *Ndrg1*$^{-/-}$ mice tended to fall sooner, the differences observed between *Ndrg1*$^{-/-}$ and *Ndrg1*$^{+/+}$ mice were less than those seen in the wire-hanging test. (C) Plot of body weights of the same mice. Mean (± standard error of the mean) body weights are shown. Each test was carried out on mice from 5 to 19 weeks of age.

pression is induced by homocysteine and reduced both the proliferation and migration rates of cultured cells (19), suggesting that NDRG4 could play a role similar to that of NDRG1 in the brain. NDRG2 and NDRG3 were expressed less in the sciatic nerve than in the brain (Fig. 7). Indeed, no apparent morphological abnormality of the brain was detected in *Ndrg1*$^{-/-}$ mice (data not shown). NDRG1 deficiency may be compensated for by other NDRG members in the brain.

Although the *Ndrg1*$^{-/-}$ mice exhibited reductive depletion of NDRG1, a nonsense mutation of human *NDRG1* (R148X) is responsible for Charcot-Marie-Tooth disease type 4D (9). The phenotypes of patients with this disease (10, 11) and of *Ndrg1*$^{-/-}$ mice in peripheral nerves were similar. This suggests that the C-terminal region of NDRG1 may be essential for NDRG1 function.

In conclusion, we found that NDRG1 deficiency leads to a peripheral neuropathy characterized by demyelination, though the initial formation of the myelin sheaths was normal. NDRG1 is abundantly expressed in the cytoplasm of Schwann cells and plays an essential role in maintenance of myelin sheaths. Although the exact molecular functions of NDRG1 are still under investigation, the *Ndrg1*$^{-/-}$ mouse will be a good model for Charcot-Marie-Tooth disease type 4D and may be used for future analysis of human peripheral nerve neuropathy as well as provide insight into potential therapies.

ACKNOWLEDGMENTS

We thank A. Nagy (Mt. Sinai Hospital) for providing R1 ES cells and *loxP* and *Cre* plasmids. We are grateful to H. Westphal (NIH) for the *EIIa-Cre* mice. We also thank Y. Imai (Riken BSI) for critical discussion.

This work was supported in part by grants-in-aid from the Ministry of Health, Labor, and Welfare of Japan and the Ministry of Education, Culture, Sports, Science, and Technology of Japan and by the Program for Promotion of Fundamental Studies in Health Science of the Organization for Pharmaceutical Safety and Research of Japan.

REFERENCES

1. **Adlkofer, K., R. Martini, A. Aguzzi, J. Zielasek, K. V. Toyka, and U. Suter.** 1995. Hypermyelination and demyelinating peripheral neuropathy in *Pmp22*-deficient mice. Nat. Genet. **11:**274–280.
2. **Agarwala, K. L., K. Kokame, H. Kato, and T. Miyata.** 2000. Phosphorylation of RTP, an ER stress-responsive cytoplasmic protein. Biochem. Biophys. Res. Commun. **272:**641–647.
3. **Bandyopadhyay, S., S. K. Pai, S. C. Gross, S. Hirota, S. Hosobe, K. Miura, K. Saito, T. Commes, S. Hayashi, M. Watabe, and K. Watabe.** 2003. The *Drg-1* gene suppresses tumor metastasis in prostate cancer. Cancer Res. **63:**1731–1736.
4. **Berger, P., P. Young, and U. Suter.** 2002. Molecular cell biology of Charcot-Marie-Tooth disease. Neurogenetics **4:**1–15.
5. **Bosboom, W. M., L. H. van den Berg, H. Franssen, P. C. Giesbergen, H. Z. Flach, A. M. van Putten, H. Veldman, and J. H. Wokke.** 2001. Diagnostic value of sural nerve demyelination in chronic inflammatory demyelinating polyneuropathy. Brain **124:**2427–2438.
6. **Guan, R. J., H. L. Ford, Y. Fu, Y. Li, L. M. Shaw, and A. B. Pardee.** 2000. Drg-1 as a differentiation-related, putative metastatic suppressor gene in human colon cancer. Cancer Res. **60:**749–755.
7. **Higashi, Y., M. Maruhashi, L. Nelles, T. Van de Putte, K. Verschueren, T. Miyoshi, A. Yoshimoto, H. Kondoh, and D. Huylebroeck.** 2002. Generation of the floxed allele of the *SIP1* (*Smad-interacting protein 1*) gene for Cre-mediated conditional knockout in the mouse. Genesis **32:**82–84.
8. **Hoogenraad, C. C., B. Koekkoek, A. Akhmanova, H. Krugers, B. Dortland, M. Miedema, A. van Alphen, W. M. Kistler, M. Jaegle, M. Koutsourakis, N. Van Camp, M. Verhoye, A. van der Linden, I. Kaverina, F. Grosveld, C. I. De Zeeuw, and N. Galjart.** 2002. Targeted mutation of *Cyln2* in the Williams syndrome critical region links CLIP-115 haploinsufficiency to neurodevelopmental abnormalities in mice. Nat. Genet. **32:**116–127.
9. **Kalaydjieva, L., D. Gresham, R. Gooding, L. Heather, F. Baas, R. de Jonge, K. Blechschmidt, D. Angelicheva, D. Chandler, P. Worsley, A. Rosenthal, R. H. King, and P. K.** 2000. Thomas. N-myc downstream-regulated gene 1 is mutated in hereditary motor and sensory neuropathy-Lom. Am. J. Hum. Genet. **67:**47–58.
10. **Kalaydjieva, L., J. Hallmayer, D. Chandler, A. Savov, A. Nikolova, D. Angelicheva, R. H. King, B. Ishpekova, K. Honeyman, F. Calafell, A. Shmarov, J. Petrova, I. Turnev, A. Hristova, M. Moskov, S. Stancheva, I. Petkova, A. H. Bittles, V. Georgieva, L. Middleton, and P. K. Thomas.** 1996. Gene mapping in Gypsies identifies a novel demyelinating neuropathy on chromosome 8q24. Nat. Genet. **14:**214–217.
11. **Kalaydjieva, L., A. Nikolova, I. Turnev, J. Petrova, A. Hristova, B. Ishpekova, I. Petkova, A. Shmarov, S. Stancheva, L. Middleton, L. Merlini, A. Trogu, J. R. Muddle, R. H. King, and P. K. Thomas.** 1998. Hereditary motor

and sensory neuropathy-Lom, a novel demyelinating neuropathy associated with deafness in gypsies. Clinical, electrophysiological and nerve biopsy findings. Brain **121:**399–408.
12. **Kokame, K., K. L. Agarwala, H. Kato, and T. Miyata.** 2000. Herp, a new ubiquitin-like membrane protein induced by endoplasmic reticulum stress. J. Biol. Chem. **275:**32846–32853.
13. **Kokame, K., H. Kato, and T. Miyata.** 1996. Homocysteine-respondent genes in vascular endothelial cells identified by differential display analysis. J. Biol. Chem. **271:**29659–29665.
14. **Kurdistani, S. K., P. Arizti, C. L. Reimer, M. M. Sugrue, S. A. Aaronson, and S. W. Lee.** 1998. Inhibition of tumor cell growth by *RTP*/*rit42* and its responsiveness to p53 and DNA damage. Cancer Res. **58:**4439–4444.
15. **Lakso, M., J. G. Pichel, J. R. Gorman, B. Sauer, Y. Okamoto, E. Lee, F. W. Alt, and H. Westphal.** 1996. Efficient in vivo manipulation of mouse genomic sequences at the zygote stage. Proc. Natl. Acad. Sci. USA **93:**5860–5865.
16. **Lin, T. M., and C. Chang.** 1997. Cloning and characterization of *TDD5*, an androgen target gene that is differentially repressed by testosterone and dihydrotestosterone. Proc. Natl. Acad. Sci. USA **94:**4988–4993.
17. **Liu, Y., A. Hoffmann, A. Grinberg, H. Westphal, M. P. McDonald, K. M. Miller, J. N. Crawley, K. Sandhoff, K. Suzuki, and R. L. Proia.** 1997. Mouse model of G_{M2} activator deficiency manifests cerebellar pathology and motor impairment. Proc. Natl. Acad. Sci. USA **94:**8138–8143.
18. **Nagy, A., J. Rossant, R. Nagy, W. Abramow-Newerly, and J. C. Roder.** 1993. Derivation of completely cell culture-derived mice from early-passage embryonic stem cells. Proc. Natl. Acad. Sci. USA **90:**8424–8428.
19. **Nishimoto, S., J. Tawara, H. Toyoda, K. Kitamura, and T. Komurasaki.** 2003. A novel homocysteine-responsive gene, smap8, modulates mitogenesis in rat vascular smooth muscle cells. Eur. J. Biochem. **270:**2521–2531.
20. **Okuda, T., and H. Kondoh.** 1999. Identification of new genes *Ndr2* and *Ndr3* which are related to *Ndr1*/*RTP*/*Drg1* but show distinct tissue specificity and response to N-myc. Biochem. Biophys. Res. Commun. **266:**208–215.
21. **Piquemal, D., D. Joulia, P. Balaguer, A. Basset, J. Marti, and T. Commes.** 1999. Differential expression of the *RTP*/*Drg1*/*Ndr1* gene product in proliferating and growth arrested cells. Biochim. Biophys. Acta **1450:**364–373.
22. **Qu, X., Y. Zhai, H. Wei, C. Zhang, G. Xing, Y. Yu, and F. He.** 2002. Characterization and expression of three novel differentiation-related genes belong to the human NDRG gene family. Mol. Cell. Biochem. **229:**35–44.
23. **Salnikow, K., W. G. An, G. Melillo, M. V. Blagosklonny, and M. Costa.** 1999. Nickel-induced transformation shifts the balance between HIF-1 and p53 transcription factors. Carcinogenesis **20:**1819–1823.
24. **Salnikow, K., T. Kluz, M. Costa, D. Piquemal, Z. N. Demidenko, K. Xie, and M. V. Blagosklonny.** 2002. The regulation of hypoxic genes by calcium involves c-Jun/AP-1, which cooperates with hypoxia-inducible factor 1 in response to hypoxia. Mol. Cell. Biol. **22:**1734–1741.
25. **Shimono, A., T. Okuda, and H. Kondoh.** 1999. N-myc-dependent repression of *Ndr1*, a gene identified by direct subtraction of whole mouse embryo cDNAs between wild type and N-*myc* mutant. Mech. Dev. **83:**39–52.
26. **Takagi, T., H. Moribe, H. Kondoh, and Y. Higashi.** 1998. DeltaEF1, a zinc finger and homeodomain transcription factor, is required for skeleton patterning in multiple lineages. Development **125:**21–31.
27. **van Belzen, N., W. N. Dinjens, M. P. Diesveld, N. A. Groen, A. C. van der Made, Y. Nozawa, R. Vlietstra, J. Trapman, and F. T. Bosman.** 1997. A novel gene which is up-regulated during colon epithelial cell differentiation and down-regulated in colorectal neoplasms. Lab. Investig. **77:**85–92.
28. **Wakisaka, Y., A. Furuta, K. Masuda, W. Morikawa, M. Kuwano, and T. Iwaki.** 2003. Cellular distribution of NDRG1 protein in the rat kidney and brain during normal postnatal development. J. Histochem. Cytochem. **51:**1515–1525.
29. **Xu, B., L. Lin, and N. S. Rote.** 1999. Identification of a stress-induced protein during human trophoblast differentiation by differential display analysis. Biol. Reprod. **61:**681–686.
30. **Yagi, T., S. Nada, N. Watanabe, H. Tamemoto, N. Kohmura, Y. Ikawa, and S. Aizawa.** 1993. A novel negative selection for homologous recombinants using diphtheria toxin A fragment gene. Anal. Biochem. **214:**77–86.
31. **Zhou, D., K. Salnikow, and M. Costa.** 1998. Cap43, a novel gene specifically induced by Ni^{2+} compounds. Cancer Res. **58:**2182–2189.
32. **Zhou, R. H., K. Kokame, Y. Tsukamoto, C. Yutani, H. Kato, and T. Miyata.** 2001. Characterization of the human NDRG gene family: a newly identified member, NDRG4, is specifically expressed in brain and heart. Genomics **73:**86–97.